Role of diatoms in nickel biogeochemistry in the ocean

Benjamin S. Twining, Stephen B. Baines, Stefan Vogt, David M Nelson

HAL Id: hal-00816929

https://hal.univ-brest.fr/hal-00816929

Submitted on 1 Nov 2021

Role of diatoms in nickel biogeochemistry in the ocean

Benjamin S. Twining,[1] Stephen B. Baines,[2] Stefan Vogt,[3] and David M. Nelson[4]

[1] Dissolved nickel (Ni) typically displays a 'nutrient-like' vertical profile in the ocean, with lower concentrations in surface waters and higher concentrations in deep waters, similar to other micronutrient metals such as iron and zinc. Vertical profiles of Ni show particular similarities to profiles of the macronutrients phosphate and silicic acid, suggesting that diatoms play an important role in mediating the vertical distribution of this metal. We performed synchrotron x-ray fluorescence (SXRF) analysis on individual phytoplankton cells collected from stations in the equatorial Pacific Ocean and from nutrient-addition incubation experiments conducted on the same cruise. Diatoms were enriched in Ni twofold to fivefold relative to picoplankton and flagellated cells. Changes in cellular quotas of Si, P and Ni observed in diatoms growing in response to Fe and Si additions were used to estimate the Ni:P (0.52 ± 0.10 mmol/mol) and Ni:Si (28 ± 13 μmol/mol) ratios of internal biomass and the frustule, respectively. Elevated internal Ni:P suggests a heightened role for urease or the Ni isoform of superoxide dismutase in diatoms (similar to cyanobacteria), while Ni associated with the frustule appears to contribute an additional 50% of cellular Ni found in the diatoms. The derived Ni:Si ratio for frustule material is comparable to Ni:Si ratios in published nutrient profiles, confirming the dominant role that diatoms play in ocean Ni biogeochemistry. While a molecular explanation for the association of Ni with frustules remains to be determined, this study demonstrates the unique biogeochemical insight that can be gained from microanalytical element analysis.

Citation: Twining, B. S., S. B. Baines, S. Vogt, and D. M. Nelson (2012), Role of diatoms in nickel biogeochemistry in the ocean, *Global Biogeochem. Cycles*, *26*, GB4001, doi:10.1029/2011GB004233.

1. Introduction

[2] Nickel is depleted in surface ocean waters and enriched at depth, displaying a 'nutrient-like' profile similar to other bioactive transition metals that are accumulated by plankton in the euphotic zone and remineralized from sinking biogenic material [*Bruland*, 1980; *Sclater et al.*, 1976]. Vertical profiles of dissolved Ni show similarities to both dissolved phosphate and silicic acid, with Ni remineralized in close stoichiometry with P in the upper water column and in close stoichiometry with Si in deeper waters [*Bruland*, 1980; *Sclater et al.*, 1976]. The correlation of Ni and P

concentrations may be explained by the sinking of either diatoms or other phytoplankton species, but the correlation of Ni and Si concentrations in bathypelagic waters suggests a specific association between these two elements in diatom frustules. Nickel bound to the opal frustules of diatoms would be expected to remineralize over longer length-scales than Ni incorporated into intracellular biochemical components. Therefore, it appears that diatoms, which mediate the biogeochemical cycling of Si in the ocean, may play a unique role in the biogeochemistry of Ni as well.

[3] The only commonly identified role for Ni in eukaryotes is urease, which catalyzes the breakdown of urea to CO_2 and NH_3 [*Frausto da Silva and Williams*, 2001]. Urea hydrolysis can also be accomplished by adenosine triphosphate urea amidolyase, which does not contain Ni, but among marine phytoplankton this enzyme has only been found in chlorophytes [*Bekheet and Syrett*, 1977; *Dyhrman and Anderson*, 2003]. Other phytoplankton growing on urea as the sole source of nitrogen have an obligate requirement for Ni [*Oliveira and Antia*, 1984; *Price and Morel*, 1991]. Further, it is known that Ni-containing superoxide dismutase (Ni-SOD) is present in some marine prokaryotes [*Eitinger*, 2004; *Palenik et al.*, 2003], and this enzyme also appears to be present in oceanic diatoms [*Cuvelier et al.*, 2010].

[1]Bigelow Laboratory for Ocean Sciences, East Boothbay, Maine, USA.
[2]Department of Ecology and Evolution, State University of New York at Stony Brook, Stony Brook, New York, USA.
[3]X-Ray Science Division, Advanced Photon Source, Argonne National Laboratory, Argonne, Illinois, USA.
[4]Institut Universitaire Européen de le Mer, Technopôle Brest-Iroise, Plouzané, France.

Corresponding author: B. S. Twining, Bigelow Laboratory for Ocean Sciences, East Boothbay, ME 04544, USA. (btwining@bigelow.org)
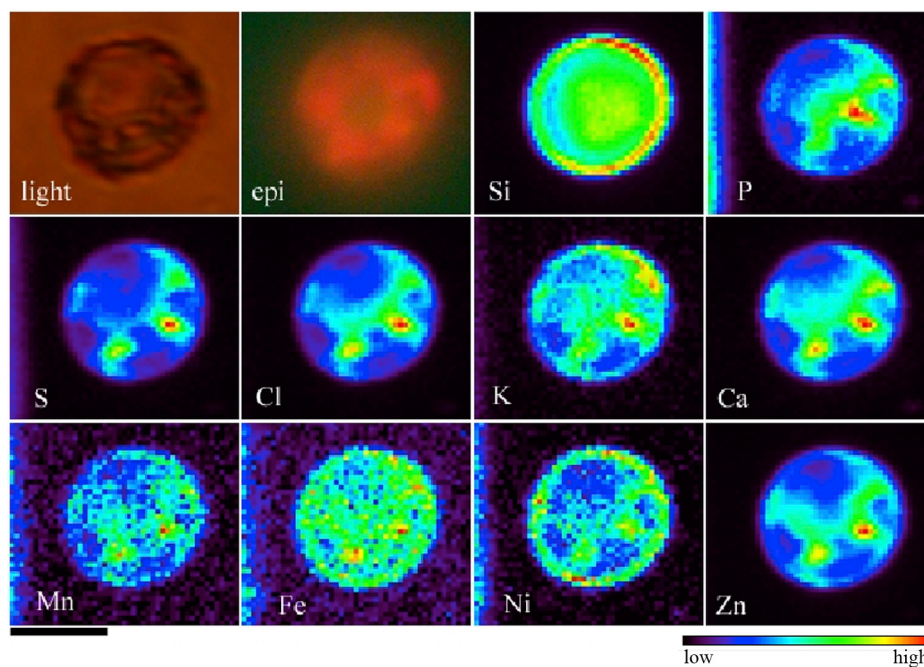
Figure 1. Light, epifluorescence and false-color SXRF element maps of a centric diatom collected from the Southern Ocean (details given in *Twining et al.* [2004]). A ring of Ni can be seen co-localized with Si around the girdle region of the cell. Iron and K also show some evidence of localization within the frustule. The scale bar is 10 μm.

[4] There are few available measurements of Ni in diatoms and other phytoplankton in the ocean. *Martin and Knauer* [1973] measured Ni:P ratios of 0.21 mmol mol^{-1} in >76-μm microplankton collected during a diatom bloom in Monterey Bay. A mixed assemblage of plankton collected from the oligotrophic North Pacific Ocean presented higher Ni:P ratios of 0.86 mmol mol^{-1} [*Collier and Edmond*, 1984]. Recent analytical advances have enabled metal quotas of individual phytoplankton cells to be measured via synchrotron x-ray fluorescence (SXRF) [*Twining et al.*, 2003]. SXRF analyses of diatoms collected from the equatorial Pacific and Southern Ocean have revealed higher Ni:P ratios in diatoms compared to non-diatoms (autotrophic and heterotrophic flagellates) [*Twining et al.*, 2004, 2011]. Furthermore, subcellular mapping of the Ni distributions in cells revealed high concentrations of Ni in the girdle area of some centric diatoms (Figure 1) [see also *Twining et al.*, 2003], suggesting a unique role for diatoms in the biogeochemical cycling of Ni.

[5] We measured changes in the Ni, P and Si content of diatoms during nutrient addition experiments in the equatorial Pacific Ocean and used the observed changes to infer the association of Ni with internal and frustule fractions of the diatoms. Using this data, we separate the contributions of frustule-bound and intracellular Ni in diatoms and compare the resulting Ni stoichiometries with those observed in non-diatoms and in published water column concentration profiles to determine the contribution of each cellular compartment of Ni cycling in the water column. These data confirm a unique and significant role of diatoms in Ni cycling and demonstrate the power of SXRF analysis to explain biogeochemical patterns and provide novel insights into marine biogeochemistry.

2. Materials and Methods

[6] Samples were collected during a cruise to the equatorial Pacific Ocean on the *R/V Roger Revelle* in December 2004. Details are given in *Twining et al.* [2011]. SXRF samples were collected from 20 to 25 m at most stations using a trace-metal clean rosette, preserved with 0.25% glutaraldehyde and centrifuged onto 200-mesh gold C/Formvar-coated TEM grids. Samples were rinsed briefly with >18 MΩ deionized water and dried. All sample preparation was performed with acid-washed plasticware in a Class-100 environment. Samples were examined using light and epifluorescence microscopy to identify appropriate target cells on the grids and to categorize cells as diatoms, autotrophic flagellated cells (Aflag), heterotrophic flagellated cells (Hflag), or autotrophic picoplankton (<2 μm; Pico).

[7] Samples were also collected from a deckboard grow-out experiment initiated at 0°N 125°W conducted in 20-L acid-washed polycarbonate carboys [*Baines et al.*, 2011]. Carboys were filled with cleanly collected unfiltered water and amended with either Fe (2 nmol L^{-1}, added as acidified FeCl$_3$), Si (20 μmol L^{-1} Si(OH)$_4$), or left unamended as a control. Carboys were incubated at ca. 50% irradiance and cooled with circulating surface seawater. SXRF analyses were performed on a subset of small pennate diatoms (similar to *Pseudo-nitzschia* sp.) that numerically dominated the biological response to the added nutrients. Ten, 11 and 17 cells were analyzed from the control, +Fe
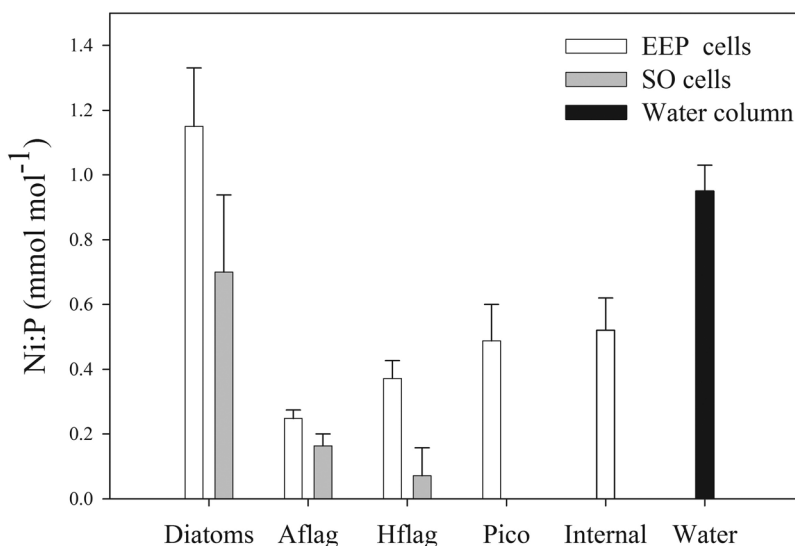
Figure 2. Ni:P ratios of cells collected from the equatorial Pacific (EEP; white bars) and Southern Ocean (SO; gray bars). Also shown is the Ni:P ratio calculated for internal cell biomass from equatorial Pacific incubations (internal) and the North Pacific Ocean water column Ni:P remineralization ratio reported by *Bruland* [1980] (water column).

and +Si carboys, respectively. Intracellular and frustule stoichiometries were calculated from differences in cell quotas between treatments as follows:

$$Ni : P_{int} = \frac{(Ni_{Fe} - Ni_{Ctrl})}{(P_{Fe} - P_{Ctrl})} \text{ and } Ni : Si_{frust} = \frac{(Ni_{Si} - Ni_{Ctrl})}{(Si_{Si} - Si_{Ctrl})}$$

where Ni:P$_{int}$ is the stoichiometry of the new cellular material synthesized following Fe addition, Ni:Si$_{frust}$ is the stoichiometry of the new deposited frustule material, and X_Y is the cellular quota (mol/cell) of element X in carboy Y (control, +Fe, or +Si) at the 96-h time point (the final time point before depletion of macronutrients [*Brzezinski et al.*, 2011]).

[8] Target cells were analyzed at the 2-ID-E hard x-ray microprobe; detailed descriptions of the instrument and technique are available elsewhere [*Twining et al.*, 2003]. Incident x-rays were tuned to energy of 10 keV and cells were scanned in 0.2–0.5 μm steps. Detector dwell times were adjusted to ensure adequate x-ray counting statistics and were typically 1–4 s. Full fluorescence spectra were collected at each pixel in the scans. Element quantification was performed as described in *Twining et al.* [2011]. Stoichiometries were log-transformed prior to statistical analysis to stabilize variance. Five out of 284 total cells were removed from the Ni data set based on low analytical signal, poor model fits to the fluorescence spectra, or significantly outlying values. Complete stoichiometric data for the cells analyzed from this cruise are reported elsewhere [*Baines et al.*, 2011; *Twining et al.*, 2011].

3. Results

[9] A total of 55 diatoms, 130 autotrophic flagellates, 82 heterotrophic flagellates, and 12 autotrophic picoplankters were used to compare Ni:P ratios in the cells collected from surface waters of the equatorial Pacific. Geometric mean

Ni:P ratios varied significantly between the four cell types, with diatoms containing significantly more Ni (relative to P) than the other plankton groups (ANOVA, $p < 0.0001$). Ni:P ratios in diatoms (1.15 ± 0.16 mmol/mol) were 4.7-, 3.1-, and 2.4-fold higher than in co-occurring autotrophic flagellates (0.25 ± 0.02 mmol/mol), heterotrophic flagellates ($0.37 + 0.05$ mmol/mol), and autotrophic picoplankton ($0.49 + 0.10$ mmol/mol), respectively (Figure 2 and Table 1). Differences between diatoms and the two flagellate groups were significant at the $p < 0.001$ level (t-test), while the diatom-picoplankton difference was weaker but still statistically significant ($p = 0.016$; t-test). Notable variations

Table 1. Ni:P and Ni:Si Stoichiometries Measured in Cells by SXRF or in Bulk Plankton With Atomic Absorption Spectrometry or Inductively Coupled Plasma Mass Spectrometry[a]

	Ni:P (mmol/mol)	Ni:Si (μmol/mol)
Equatorial Pacific		
Diatoms	1.15 ± 0.16	74 ± 9
Aflag	0.25 ± 0.02	–
Hflag	0.37 ± 0.05	–
Pico	0.49 ± 0.10	–
Southern Ocean		
Diatoms	0.70 ± 0.21	11 ± 3
Aflag	0.16 ± 0.03	–
Hflag	0.07 ± 0.06	–
Bulk Plankton		
Twining et al. [2011][b]	1.08 ± 0.41	–
Bruland et al. [1991][c]	0.47 ± 0.35	–
Cellular Fractions Calculated From Carboy Experiments		
+Fe biomass change	0.52 ± 0.10	–
+Si biomass change	–	28 ± 13

[a]SXRF data from the Equatorial Pacific and Southern Ocean are geometric means $\pm$ SE. For the carboy data errors are propagated SE.
[b]>3-μm plankton collected from equatorial Pacific Ocean.
[c]>0.45-μm plankton collected from equatorial and coastal Pacific Ocean.
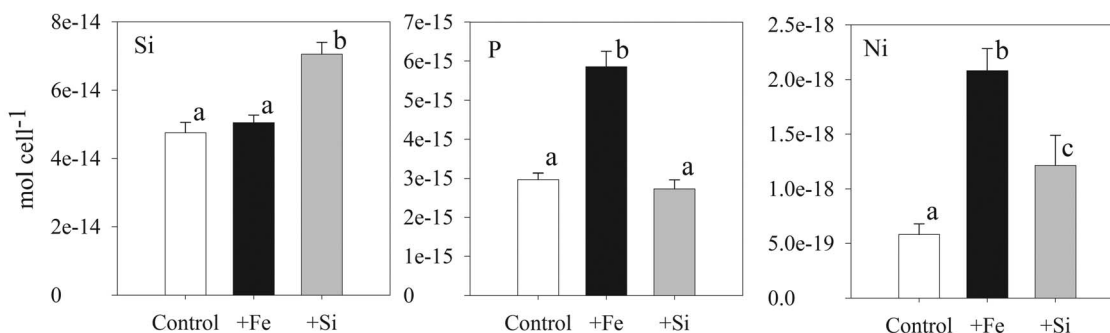
Figure 3. Cellular quotas (mol/cell) of Si, P and Ni in a single morphotype of pennate diatom collected from treatments (unamended control [white bar], +Fe [black bar], +Si [gray bar]) of a deckboard incubation experiment conducted in the equatorial Pacific Ocean. Bars are geometric mean (±SE) element quotas of cells collected at the 96-h time point. Treatment means found to be significantly different with paired t-tests ($p < 0.05$) are indicated with unique letters above the bars.

were also observed between non-diatom taxa, with autotrophic picoplankton and heterotrophic flagellates both containing more Ni than autotrophic flagellates (t-test; $p = 0.045$ and 0.010, respectively).

[10] The addition of Fe stimulated the growth of larger (>3 μm) phytoplankton in the carboy experiment, while no significant changes in 0.45–3 μm chlorophyll concentrations were observed [Brzezinski et al., 2011]. Diatoms dominated the biomass response in the Fe-amended carboys, however the addition of silicic acid did not enhance chlorophyll concentrations in either size class [Brzezinski et al., 2011]. The visual appearance and cell length of diatoms in the carboys were constant across treatments, but cell width increased in response to nutrient additions, driving 77% and 50% increases in cell volume in response to Fe and Si, respectively [Baines et al., 2011]. The elemental content of the diatoms changed significantly in response to both added Fe and silicic acid (Figure 3). After 96 h of incubation, cellular P increased ca. twofold in diatoms from the +Fe carboy (5.9 ± 0.4 fmol cell^{-1}) compared to diatoms from the control (3.0 ± 0.2 fmol cell^{-1}), but Si addition did not result in significant changes in cellular P (2.7 ± 0.2 fmol cell^{-1}). Conversely, cellular Si increased approximately 50% over 4 days in response to added Si (71 ± 3 fmol cell^{-1} in +Si compared to 48 ± 3 fmol cell^{-1} in control) but showed no significant response to added Fe (51 ± 2 fmol cell^{-1}). In contrast with the major elements, Ni increased in diatoms in response to both Si and Fe additions, with cellular Ni increasing 3.6 and 2.1-fold relative to the control (0.58 ± 0.09 amol cell^{-1}) in cells collected at 96 h from Fe- (2.08 ± 0.19 amol/cell) and Si-amended carboys (1.21 ± 0.25 amol cell^{-1}), respectively. The cellular quotas were used to calculate the Ni stoichiometries of the intracellular (Ni:$P_{int} = 0.52 \pm 0.10$ mmol/mol) and frustule (Ni:$Si_{frust} = 28 \pm 13$ μmol/mol) cellular fractions.

4. Discussion

4.1. Nickel Associations With Diatoms

[11] Diatoms collected from the equatorial Pacific Ocean had significantly higher Ni:P ratios than other co-occurring cell types. Elevated diatom Ni:P ratios were also documented with SXRF analyses in the Southern Ocean, where diatom Ni:P ratios were 4.3- and 9.9-fold higher than in co-occurring autotrophic and heterotrophic flagellates (Figure 2) [Twining et al., 2004]. To our knowledge, these are the first published reports of systematically elevated Ni in diatoms from either laboratory or field studies. Ratios of Ni:P have been reported for suspended marine particulate material (0.21–0.86 mmol/mol [Bruland et al., 1991]), and these bulk ratios fall between the ratios measured in the various cell types with SXRF.

[12] To investigate the possible drivers of elevated Ni content in diatoms, cell quotas were divided into internal and frustule-associated fractions by examining the response of cells to added Fe and Si in the carboy incubations. The pennate diatoms produced more intracellular biomass (e.g., ribosomes, mitochondria, cytosol) in response to Fe but did not alter silicification. The increases in intracellular biomass are shown by changes in P quotas (Figure 3), as well as by changes in cellular S. Sulfur is primarily associated with cysteine and methionine moieties within proteins or polyamines [Roberts et al., 1955] and can be used as an alternate biomass proxy [Baines et al., 2011]. Although S can also be found as dimethylsulfoniopropionate (DMSP) in diatoms under Fe stress [Sunda et al., 2002], the diatoms in these incubations had been released from Fe limitation, and thus cellular DMSP would be expected to decrease rather than increase. Sulfur quotas showed no change in the control treatment during the incubations but increased 2.4-fold in response to Fe (9.9 ± 0.8 fmol S cell^{-1} in + Fe compared to 4.1 ± 0.2 fmol S cell^{-1} in control), similar to P. Therefore the observed increases in Ni cell^{-1} are taken as broadly representative of the Ni:P stoichiometry of the internal organic matter of the diatoms. Similarly, diatoms deposited more opal into their frustules in response to silicate additions but did not synthesize more internal biomass As with P, S quotas were essentially unchanged in response to Si (4.6 ± 0.3 fmol cell^{-1} in + Si compared to 4.1 ± 0.2 fmol cell^{-1} in control) [Baines et al., 2011]. Therefore the observed increases in Ni cell^{-1} are interpreted as representative of the Ni:Si stoichiometry of the diatom frustule.

[13] As a check on the consistency of the Ni:P and Ni:Si ratios derived from the incubation experiment, these ratios were used to calculate Ni quotas for diatoms collected from stations across and along the equator in the Pacific Ocean. Ni

quotas (mol cell^{-1}) for these cells were estimated by multiplying Ni:P$_{int}$ by the cell-specific P quota (mol cell^{-1}) and Ni:Si$_{frust}$ by the cell-specific Si quota (mol cell^{-1}). Calculated Ni quotas were, on average, $85 \pm 8\%$ (1 SE) of the measured Ni quotas, and 'internal' and 'frustule' Ni each accounted for $50 \pm 1\%$ of the total cellular Ni. As an additional check on the derived Ni ratios, the Ni:P of the intracellular material added by the diatoms (Ni:P$_{int}$ = 0.52 ± 0.10 mmol/mol) was 41% of the whole-cell Ni:P ratios of these diatoms at the start of the incubation experiment (1.27 ± 0.35 mmol/mol), similar (within error) to the approximately 50% fraction of Ni estimated to be associated with intracellular biomass of equatorial Pacific diatoms. It thus appears that there are two distinct fractions of Ni in diatoms: Ni associated with intracellular machinery and Ni associated with the frustule.

[14] Internal Ni comprised only half of the Ni associated with equatorial Pacific diatoms, but Ni:P$_{int}$ alone was still higher than whole-cell Ni:P ratios observed in most nondiatoms from the equatorial Pacific and Southern Ocean. In fact, Ni:P$_{int}$ of diatoms was comparable to mean whole-cell Ni:P measured in cyanobacteria in the equatorial Pacific, which was itself higher than in larger flagellated photoautotrophs (Figure 2). Elevated Ni content of cyanobacteria has been reported in freshwater species [*Ji and Sherrell*, 2008] and may result from an elevated importance of Ni-SOD to cyanobacterial physiology. Ni-SOD is the only SOD isoform present in all sequenced strains of *Prochlorococcus*, as well as in at least one strain of *Synechococcus* [*Dupont et al.*, 2008a]. Ni-SOD is a recently evolved enzyme that appears to have been shared between phyologenetic groups via horizontal gene transfer, and the presence of Ni-SOD in cyanobacteria is always associated with the loss of the Fe isoform of SOD [*Dupont et al.*, 2008a, 2008b; *Schmidt et al.*, 2009]. It has thus been suggested that Ni-SOD may have evolved in response to low Fe availability in the modern ocean [*Dupont et al.*, 2008b]. Open-ocean diatom strains contain Ni-SOD as well [*Cuvelier et al.*, 2010], and elevated Ni:P$_{int}$ may reflect preferential usage of Ni-SOD by diatoms relative to other eukaryotic taxa. However, Mn-SOD is also present in diatoms [*Wolfe-Simon et al.*, 2005], and diatoms appear to produce more Mn-SOD under Fe stress [*Peers and Price*, 2004]. Further research is needed to ascertain the importance of Ni-SOD to diatoms.

[15] The elevated Ni:P$_{int}$ of diatoms may indicate that diatoms are supporting growth through uptake and utilization of DON via urease. Indeed, studies in the equatorial Pacific have concluded that diatoms in this region utilize organic N as growth substrate [*Price et al.*, 1991, 1994], and work performed on the same cruise demonstrated rapid diatom growth rates and *f*-ratios of larger cells between 0.27 and 0.41 [*Parker et al.*, 2011; *Selph et al.*, 2011], indicating that the growth of larger cells such as diatoms is substantially supported by recycled N. However, nitrate utilization was stimulated in the same +Fe incubations in which elevated diatom Ni:P was observed [*Brzezinski et al.*, 2011], and urease may be expressed constitutively [*Allen et al.*, 2011] or even up-regulated by diatoms growing on nitrate [*Peers et al.*, 2000]. Thus, the presence of elevated urease, if observed, may be an equivocal indicator of DON utilization.

[16] Alternatively, *Allen et al.* [2011] demonstrated that diatoms use an ornithine-urea cycle to enhance their response to episodic N availability. They found that urease levels in the pennate diatom *Phaeodactylum tricornutum* did not change in response to pulsed N inputs but were consistently elevated. *Peers et al.* [2000] also found urease to be constitutively expressed in two centric diatom species. Thus, the apparently unique role played by the ornithine-urea cycle in diatom physiology, as well as elevated constitutive expression of urease in these organisms, may provide an alternate explanation for the relatively high intracellular Ni:P ratios in diatoms. Furthermore, *Dupont et al.* [2010] suggested that Fe and Ni membrane transporters may compete for surface area in larger cells such as diatoms. They proposed that additions of Fe to Fe-limited phytoplankton should result in the accumulation of Ni, as observed here. It is evident that there are several possible explanations for the elevated intracellular Ni:P ratios of diatoms which remain to be tested.

[17] Maps of Ni in diatoms (Figure 1) [*Twining et al.*, 2003], as well as the incorporation of additional Ni during diatom silicification, confirm that Ni is also associated with the silica frustule. However, the mechanism by which Ni is incorporated into the frustule has yet to be determined. Silica is polymerized and formed into the intricate nano-scaffold of the frustule within the silica deposition vesicle [*Hildebrand*, 2008; *Round et al.*, 1990], and thus non-specific absorption of ambient dissolved Ni into the frustule during polymeriziation [e.g., *Sheng et al.*, 2011] seems unlikely. It is more likely that Ni is contained in biochemical moieties associated with the frustule or is involved in the biochemical processes required to precipitate the frustule and becomes inadvertently trapped within the frustule. It is possible that frustule-associated Ni is contained in ureases spanning the silicalemma of the silica deposition vesicle (SDV). A portion of cellular urease is localized to the outer membrane of some bacterial strains [*Baik et al.*, 2004; *Mclean et al.*, 1985; *Phadnis et al.*, 1996], but in other bacterial strains and in plants urease is present primarily in the cytoplasm [*Faye et al.*, 1986; *Mobley and Hausinger*, 1989; *Mobley et al.*, 1995]. If present, frustule-associated Ni which is actually contained in membrane-bound ureases could be preferentially preserved by the opal test during water column remineralization. For example, it has been shown that organic molecules such as proteins and amino acids are intimately associated with silica in frustules [*Abramson et al.*, 2009].

[18] Researchers have identified several groups of proteins involved in frustule formation, including frustulins and silaffins [*Kröger et al.*, 1996, 1999], and long-chain polyamines are also known to be associated with frustule formation [*Sumper and Kröger*, 2004]. Silaffin-like proteins are intimately associated with silica in the frustule [*Scheffel et al.*, 2011]. The long-chain polyamines are composed of precursors such as putrescine and ornithine that are produced by the cellular urea cycle. However, urease serves to reduce ornithine production by the urea cycle, lowering concentrations of the precursor of the long-chain polyamines involved in silica polymerization. Thus it is not clear why urease production would increase in concert with heightened silicification. Alternately, urease may be used to adjust pH in support of frustule formation. Urease is used by some bacteria to raise the pH of acid environments [*Huynh and Grinstein*, 2007]. While the SDV is thought to provide an acidic environment to support silica polymerization [*Vrieling*

Table 2. Dissolved Ni:P and Ni:Si Concentration Ratios Reported in Previous Studies in the North Pacific Ocean and Indian Ocean[a]

	Latitude	Longitude	Ni:P (mmol/mol)	Ni:Si (μmol/mol)	r^2
		North Pacific Ocean			
Bruland [1980] Sta. H-77	32° 41′ N	144° 59.5′ W	**0.83 $\pm$ 0.12**	**35 $\pm$ 2**	0.996
Sclater et al. [1976] Sta. 204	31° 23′ N	150° 2′ W	1.17 $\pm$ 0.55	**26 $\pm$ 9**	0.949
Sclater et al. [1976] Sta. 343	16° 32′ N	123° 1′ W	**1.03 $\pm$ 0.25**	**37 $\pm$ 4**	0.949
North Pacific average			1.01 $\pm$ 0.17	33 $\pm$ 6	
		Indian Ocean			
Saager et al. [1992] Sta. 5	14° 30′ N	67° E	**0.58 $\pm$ 0.34**	**41 $\pm$ 5**	0.917
Saager et al. [1992] Sta. 6	19° N	67° E	0.38 $\pm$ 0.35	**69 $\pm$ 6**	0.946
Saager et al. [1992] Sta. 7	21° 16′ N	63° 22′ E	0.40 $\pm$ 0.45	**46 $\pm$ 6**	0.907
Morley et al. [1993] Sta. 2	12° 14.9′ S	55° 2.2′ E	0.48 $\pm$ 0.50	**23 $\pm$ 8**	0.847
Morley et al. [1993] Sta. 3	18° 36.7′ S	55° 36.2′ E	**1.97 $\pm$ 0.13**	9 $\pm$ 2	0.993
Morley et al. [1993] Sta. 4	27° 0.5′ S	56° 58′ E	**2.03 $\pm$ 0.28**	6 $\pm$ 4	0.922
Morley et al. [1993] Sta. 6	8° 27.4′ S	52° 43.9′ E	**1.64 $\pm$ 0.71**	**22 $\pm$ 7**	0.957
Morley et al. [1993] Sta. 7	6° 9.2′ S	50° 53.7′ E	**1.65 $\pm$ 0.30**	9 $\pm$ 6	0.892
Indian Ocean average			1.14 $\pm$ 0.74	28 $\pm$ 22	

[a]Ratios were calculated by multiple linear regression of Ni against P and Si. Data from all depths above the deep silicic acid maximum (typically ca. 3,500 m) were used in the regressions. Parameters are presented $\pm$ standard error calculated from individual fitting of each station. Parameters shown in bold are statistically significant ($p < 0.05$). The average ($\pm$SD) Ni:P and Ni:Si for each ocean basin is also shown.

et al., 1999], diatoms may need to adjust pH upward at some point during silicification, perhaps to maintain silicic acid in solution at high concentrations prior to polymerization or to adjust SDV pH following frustule formation. A mechanistic molecular explanation for the role of Ni in frustule formation remains to be determined, but we postulate that urease plays some role in silica polymerization and could become associated with the completed frustule as a result.

4.2. Comparisons With Water Column Ni Distributions

[19] Our finding of separate associations of Ni with the internal and frustule fractions of diatoms is consistent with distributions of dissolved P, Si and Ni in the water column. Vertical profiles of these nutrients from the Atlantic, Pacific and Indian Oceans show a correspondence of Ni concentrations with both phosphate and silicic acid [*Bruland*, 1980; *Morley et al.*, 1993; *Saager et al.*, 1992; *Sclater et al.*, 1976]. Both *Sclater et al.* [1976] and *Bruland* [1980] used multiple linear regression to estimate ratios of Ni:P and Ni:Si in the water column, and we have extended this analysis to open-ocean stations in the Indian Ocean (Table 2). Coefficients of determination (r^2) range from 0.892 to 0.996, demonstrating the close relationship between these dissolved nutrients. Data from the two North Pacific studies show relatively close agreement in both ratios, while the Indian Ocean studies differ in the relative magnitude of Ni:P and Ni:Si. Stations sampled by *Saager et al.* [1992] have relatively low Ni:P (0.38–0.58 mmol/mol) and relatively high Ni:Si (41–69 μmol/mol), while stations sampled by *Morley et al.* [1993] have approximately fourfold higher Ni:P (0.48–2.03 mmol/mol) but approximately fourfold lower Ni:Si (6–23 μmol/mol) than observed by *Saager et al.* [1992].

[20] This may indicate real differences in the cycling of Ni in these areas (although they are both in tropical waters of the western Indian Ocean), but it could also result from analytical differences between the studies that favor one ratio at the expense of the other. All three nutrients are remineralized in the upper 1,000 m of the water column, and the estimated Ni:Si ratio is therefore constrained largely by the relationship between these elements in the deeper waters (as P is remineralized nearly entirely in the upper 1,000 m). The regression model adjusts the estimated Ni:P ratio to best match the upper water column nutrient data within the constraints of the Ni:Si ratio, and therefore the two ratios are negatively correlated with each other across the entire data set. The regression models show that Si is a significantly better predictor of Ni than is P (based on partial sums of squares). Therefore, the differences between the Indian Ocean studies may represent differences in the deep-water remineralization of Ni and Si, with Ni:P estimates changing in response. Statistical comparisons show that differences between studies are more significant than differences between stations, also suggesting that methodological differences may be at play here. In spite of (or perhaps because of) the variations discussed above, mean ($\pm$SD) Ni:P and Ni:Si ratios for North Pacific and Indian Ocean stations are not significantly different from each other.

[21] Comparisons of water column Ni ratios with those in diatoms and other plankton suggest roles for each in Ni export. Based on the close agreement of ocean Ni:Si ratios with that calculated for the frustule fraction of diatoms in the carboy experiments, diatoms appear to be primarily responsible for Ni export to deep waters. However, the situation in the upper water column is less clear. Average water column Ni:P ratios are similar to those in whole diatoms but are twofold above that estimated for internal diatom biomass (0.52 $\pm$ 0.10 mmol/mol), which is the fraction assumed to affect Ni:P ratios in the upper 1,000 m where nearly all P remineralization takes place (Table 3). The offset in water column Ni:P may be explained by Ni uptake and remineralization by other plankton with yet higher Ni:P ratios. *Synechococcus* have elevated Ni:P compared to autotrophic flagellates (Table 1), and work in the North Atlantic has shown *Synechococcus* Ni:P to increase by nearly an order of magnitude (up to 3.40 mmol/mol) in response to nutrient delivery in mesoscale eddies [*Twining et al.*, 2010]. Cyanobacteria are far more abundant than diatoms in open-ocean settings and may contribute to organic matter export

Table 3. Comparison of Remineralization of Ni From Sinking Phytoplankton in the Pacific Ocean and Indian Ocean as Measured in the Studies Presented in Table 2 or Calculated From Remineralized Si and P in Each Study Using Ni:Si$_{frust}$ and Ni:P$_{int}$ for Frustule- and Cytosol-Associated Ni Measured in This Study[a]

	Measured Remineralization				Calculated Remineralization				
	P max (m)	P (μM)	Si (μM)	Ni (nM)	Ni From Cytosol (nM)	Ni From Frustule (nM)	Total Ni (nM)	Calculated/ Measured	Percent From Frustule
North Pacific Ocean									
Bruland [1980] Sta. H-77	985	3.3	126	7.2	1.7	3.5	5.2	72%	67%
	–	–	39	1.3	–	1.1	1.1	85%	–
Sclater et al. [1976] Sta. 204	1,039	3.2	128	6.4	1.6	3.5	5.2	81%	68%
	–	–	44	1.8	–	1.2	1.2	67%	–
Sclater et al. [1976] Sta. 343	791	2.9	86	5.2	1.5	2.4	3.9	75%	61%
	–	–	72	2.9	–	2.0	2.0	69%	–
Indian Ocean									
Saager et al. [1992] Sta. 6	1,200	2.0	74	5.7	1.0	2.0	3.1	54%	67%
	–	–	43	3.9	–	1.2	1.2	31%	–
Saager et al. [1992] Sta. 7	1,600	2.4	124	6.7	1.3	3.4	4.7	69%	73%
	–	–	64	2.8	–	1.8	1.8	64%	—
Morley et al. [1993] Sta. 3	1,000	2.1	66	4.2	1.1	1.8	2.9	69%	63%
	–	–	64	0.5	–	1.8	1.8	352%	–
Morley et al. [1993] Sta. 7	965	2.7	79	4.2	1.4	2.2	3.6	85%	61%
	–	–	58	0.4	–	1.6	1.6	400%	–

[a]For each station, remineralization calculations have been performed for two regions of the water column. The first row for each station shows nutrient remineralization in the upper water column down to the depth of the maximum phosphate concentration (shown in the second column), and the second row shows nutrient remineralization from the depth of the phosphate maximum to the depth of the silicic acid maximum. Upper water column remineralization was calculated by subtracting nutrient concentrations in surface waters from those at the P maximum, and lower water column remineralization was calculated by subtracting nutrient concentrations at the depth of maximum P concentration from those at the depth of maximum Si concentration. The final column shows the percentage of calculated upper water column remineralization which is predicted to come from the dissolution of diatom frustules.

as well [*Amacher et al.*, 2009; *Lomas and Moran*, 2011; *Richardson and Jackson*, 2007]. Heterotrophic bacteria contain Ni-SOD, and some groups have additional Ni proteins involved in methanogenesis [*Ragsdale*, 2009]. As a result, heterotrophic bacteria are likely to have elevated Ni quotas and may contribute to Ni cycling in the upper water column as a food source for heterotrophic protists and through associations with sinking organic aggregates.

[22] As an alternate approach to examine the role of diatoms in Ni export, we attempted to reproduce the Ni remineralization patterns measured in the North Pacific and Indian Ocean using our estimates of Ni:P$_{int}$ and Ni:Si$_{frust}$ (Table 3) Concentrations of remineralized phosphate and silicic acid were calculated for the upper water column (above the phosphate maximum) and the lower water column (between the phosphate maximum and silicic acid maximum). These were multiplied by the Ni:P$_{int}$ and Ni:Si$_{frust}$ ratios derived from the carboy experiment, and calculated remineralized Ni was compared to measured levels for these depth regions. Calculated Ni remineralized in the upper water column was consistently ca. 30% below measured Ni remineralization values. This suggests that Ni:P$_{int}$ may be underestimated by the carboy experiment results (matching the finding of the Ni quota reconstructions discussed previously), and/or that other groups with elevated Ni:P also make significant contributions to Ni flux in the upper water column, as discussed above. In the lower water column, comparisons between calculated and measured values were more variable. In the North Pacific calculated deep water values were about 25% below measured values, but in the Indian measured Ni remineralization ranged from 31% to 400% of measured values. These large discrepancies could be an artifact of relatively small changes in dissolved Ni in the deeper waters (making the calculations more vulnerable to analytical error). They could also be driven by water mass differences, as deep waters are transported laterally via thermohaline circulation and have only partial biogeochemical connection with the overlying waters. It is also interesting to note that although diatoms clearly export Ni to deep waters, frustules are an important source of Ni in the upper 1,000 m as well. Comparison of Ni remineralization from diatom cytosol to Ni remineralization from frustules shows that frustules consistently account for about 2/3 of upper water column remineralization. This follows from the observation that typically 50–75% of all Si remineralization occurs in the upper water column.

[23] The measurements of Ni, P and Si in diatoms and other plankton from the equatorial Pacific presented here point to an important role for diatoms as mediators of sinking Ni flux in the ocean. This role results both from elevated internal Ni levels in diatoms relative to other eukaryotes, as well as from a unique association between Ni and the opal frustule of diatoms. Diatom Ni flux may be augmented by the sinking of other high-Ni groups such as cyanobacteria and heterotrophic bacteria. While this work clearly implicates diatoms in the ocean Ni cycle, we do not yet have a molecular understanding for the causes of the elevated Ni content of diatoms. High internal Ni:P in diatoms may result from enhanced usage of urease and Ni-SOD, like cyanobacteria, or a Ni protein yet to be identified. The association of Ni with the diatom frustule remains unexplained, as well. Application of genomic and proteomic tools to address these questions should further advance our understanding of the roles of individual plankton groups in ocean trace metal cycles.

References

Abramson, L., S. Wirick, C. Lee, C. Jacobsen, and J. A. Brandes (2009), The use of soft X-ray spectromicroscopy to investigate the distribution and composition of organic matter in a diatom frustule and a biomimetic analog, *Deep Sea Res., Part II*, 56, 1369–1380, doi:10.1016/j.dsr2.2008.11.031.

Allen, A. E., et al. (2011), Evolution and metabolic significance of the urea cycle in photosynthetic diatoms, *Nature*, 473(7346), 203–207, doi:10.1038/nature10074.

Amacher, J., S. Neuer, I. Anderson, and R. Massana (2009), Molecular approach to determine contributions of the protist community to particle flux, *Deep Sea Res., Part I*, 56(12), 2206–2215, doi:10.1016/j.dsr.2009.08.007.

Baik, S. C., et al. (2004), Proteomic analysis of the sarcosine-insoluble outer membrane fraction of *Helicobacter pylori* strain 26695, *J. Bacteriol.*, 186(4), 949–955, doi:10.1128/JB.186.4.949-955.2004.

Baines, S. B., B. S. Twining, S. Vogt, W. M. Balch, N. S. Fisher, and D. M. Nelson (2011), Elemental composition of equatorial Pacific diatoms exposed to additions of silicic acid and iron, *Deep Sea Res., Part II*, 58, 512–523, doi:10.1016/j.dsr2.2010.08.003.

Bekheet, J. A., and P. J. Syrett (1977), Urea-degrading enzymes in algae, *Br. Phycol. J.*, 12, 137–143, doi:10.1080/00071617700650151.

Bruland, K. W. (1980), Oceanographic distributions of cadmium, zinc, nickel, and copper in the North Pacific, *Earth Planet. Sci. Lett.*, 47(2), 176–198, doi:10.1016/0012-821X(80)90035-7.

Bruland, K. W., J. R. Donat, and D. A. Hutchins (1991), Interactive influences of bioactive trace-metals on biological production in oceanic waters, *Limnol. Oceanogr.*, 36(8), 1555–1577, doi:10.4319/lo.1991.36.8.1555.

Brzezinski, M. A., et al. (2011), Co-limitation of diatoms by iron and silicic acid in the equatorial Pacific, *Deep Sea Res., Part II*, 58(3–4), 493–511, doi:10.1016/j.dsr2.2010.08.005.

Collier, R., and J. Edmond (1984), The trace element geochemistry of marine biogenic particulate matter, *Prog. Oceanogr.*, 13(2), 113–199, doi:10.1016/0079-6611(84)90008-9.

Cuvelier, M. L., et al. (2010), Targeted metagenomics and ecology of globally important uncultured eukaryotic phytoplankton, *Proc. Natl. Acad. Sci. U. S. A.*, 107(33), 14,679–14,684, doi:10.1073/pnas.1001665107.

Dupont, C. L., K. Barbeau, and B. Palenik (2008a), Ni uptake and limitation in marine *Synechococcus* strains, *Appl. Environ. Microbiol.*, 74(1), 23–31, doi:10.1128/AEM.01007-07.

Dupont, C. L., K. Neupane, J. Shearer, and B. Palenik (2008b), Diversity, function and evolution of genes coding for putative Ni-containing superoxide dismutases, *Environ. Microbiol.*, 10(7), 1831–1843, doi:10.1111/j.1462-2920.2008.01604.x.

Dupont, C. L., K. N. Buck, B. Palenik, and K. Barbeau (2010), Nickel utilization in phytoplankton assemblages from contrasting oceanic regimes, *Deep Sea Res., Part I*, 57, 553–566, doi:10.1016/j.dsr.2009.12.014.

Dyhrman, S. T., and D. M. Anderson (2003), Urease activity in cultures and field populations of the toxic dinoflagellate *Alexandrium*, *Limnol. Oceanogr.*, 48(2), 647–655, doi:10.4319/lo.2003.48.2.0647.

Eitinger, T. (2004), In vivo production of active nickel superoxide dismutase from *Prochlorococcus marinus* MIT9313 is dependent on its cognate peptidase, *J. Bacteriol.*, 186(22), 7821–7825, doi:10.1128/JB.186.22.7821-7825.2004.

Faye, L., J. S. Greenwood, and M. J. Chrispeels (1986), Urease in Jack-Bean (*Canavalia ensiformis* (L) DC) seeds is a cytosolic protein, *Planta*, 168(4), 579–585, doi:10.1007/BF00392279.

Frausto da Silva, J. R. R., and R. J. P. Williams (2001), *The Biological Chemistry of the Elements: The Inorganic Chemistry of Life*, 2nd ed., 575 pp., Oxford Univ. Press, Oxford, U. K.

Hildebrand, M. (2008), Diatoms, biomineralization processes, and genomics, *Chem. Rev.*, 108(11), 4855–4874, doi:10.1021/cr078252z.

Huynh, K. K., and S. Grinstein (2007), Regulation of vacuolar pH and its modulation by some microbial species, *Microbiol. Mol. Biol. Rev.*, 71(3), 452–462, doi:10.1128/MMBR.00003-07.

Ji, Y. C., and R. M. Sherrell (2008), Differential effects of phosphorus limitation on cellular metals in *Chlorella* and *Microcystis*, *Limnol. Oceanogr.*, 53(5), 1790–1804, doi:10.4319/lo.2008.53.5.1790.

Kröger, N., C. Bergsdorf, and M. Sumper (1996), Frustulins: Domain conservation in a protein family associated with diatom cell walls, *Eur. J. Biochem.*, 239(2), 259–264, doi:10.1111/j.1432-1033.1996.0259u.x.

Kröger, N., R. Deutzmann, and M. Sumper (1999), Polycationic peptides from diatom biosilica that direct silica nanosphere formation, *Science*, 286(5442), 1129–1132, doi:10.1126/science.286.5442.1129.

Lomas, M. W., and S. B. Moran (2011), Evidence for aggregation and export of cyanobacteria and nano-eukaryotes from the Sargasso Sea euphotic zone, *Biogeosciences*, 8, 203–216, doi:10.5194/bg-8-203-2011.

Martin, J. H., and G. A. Knauer (1973), The elemental composition of plankton, *Geochim. Cosmochim. Acta*, 37, 1639–1653, doi:10.1016/0016-7037(73)90154-3.

Mclean, R. J. C., K. J. Cheng, W. D. Gould, and J. W. Costerton (1985), Cytochemical localization of urease in a rumen *Staphylococcus* sp. by electron microscopy, *Appl. Environ. Microbiol.*, 49(1), 253–255.

Mobley, H. L. T., and R. P. Hausinger (1989), Microbial ureases: Significance, regulation, and molecular characterization, *Microbiol. Rev.*, 53(1), 85–108.

Mobley, H. L. T., M. D. Island, and R. P. Hausinger (1995), Molecular biology of microbial ureases, *Microbiol. Rev.*, 59(3), 451–480.

Morley, N. H., P. J. Statham, and J. D. Burton (1993), Dissolved trace metals in the southwestern Indian Ocean, *Deep Sea Res., Part I*, 40(5), 1043–1062, doi:10.1016/0967-0637(93)90089-L.

Oliveira, L., and N. J. Antia (1984), Evidence of nickel ion requirement for autotrophic growth of a marine diatom with urea serving as nitrogen source, *Br. Phycol. J.*, 19(2), 125–134, doi:10.1080/00071618400650131.

Palenik, B., et al. (2003), The genome of a motile marine *Synechococcus*, *Nature*, 424, 1037–1042, doi:10.1038/nature01943.

Parker, A. E., F. P. Wilkerson, R. C. Dugdale, A. M. Marchi, V. E. Hogue, M. R. Landry, and A. G. Taylor (2011), Spatial patterns of nitrogen uptake and phytoplankton in the equatorial upwelling zone (110°W–140°W) during 2004 and 2005, *Deep Sea Res., Part II*, 58(3–4), 417–433, doi:10.1016/j.dsr2.2010.08.013.

Peers, G., and N. M. Price (2004), A role for manganese in superoxide dismutases and growth of iron-deficient diatoms, *Limnol. Oceanogr.*, 49(5), 1774–1783, doi:10.4319/lo.2004.49.5.1774.

Peers, G. S., A. J. Milligan, and P. J. Harrison (2000), Assay optimization and regulation of urease activity in two marine diatoms, *J. Phycol.*, 36, 523–528, doi:10.1046/j.1529-8817.2000.99037.x.

Phadnis, S. H., M. H. Parlow, M. Levy, D. Ilver, C. M. Caulkins, J. B. Connors, and B. E. Dunn (1996), Surface localization of *Helicobacter pylori* urease and a heat shock protein homolog requires bacterial autolysis, *Infect. Immun.*, 64(3), 905–912.

Price, N. M., and F. M. M. Morel (1991), Colimitation of phytoplankton growth by nickel and nitrogen, *Limnol. Oceanogr.*, 36, 1071–1077, doi:10.4319/lo.1991.36.6.1071.

Price, N. M., L. F. Andersen, and F. M. M. Morel (1991), Iron and nitrogen nutrition of equatorial Pacific plankton, *Deep Sea Res.*, 38(11), 1361–1378, doi:10.1016/0198-0149(91)90011-4.

Price, N. M., B. A. Ahner, and F. M. M. Morel (1994), The equatorial Pacific Ocean: Grazer-controlled phytoplankton populations in an iron-limited ecosystem, *Limnol. Oceanogr.*, 39(3), 520–534, doi:10.4319/lo.1994.39.3.0520.

Ragsdale, S. W. (2009), Nickel-based enzyme systems, *J. Biol. Chem.*, 284(28), 18,571–18,575, doi:10.1074/jbc.R900020200.

Richardson, T. L., and G. A. Jackson (2007), Small phytoplankton and carbon export from the surface ocean, *Science*, 315(5813), 838–840, doi:10.1126/science.1133471.

Roberts, R. B., D. B. Cowie, P. H. Abelson, E. T. Bolton, and R. V. Britten (1955), *Studies in Biosynthesis in Escherichia coli*, 551 pp., Carnegie Inst. of Wash., Washington, D. C.

Round, F. E., R. M. Crawford, and D. G. Mann (1990), *The Diatoms: Biology and Morphology of the Genera*, 747 pp., Cambridge Univ. Press, Cambridge, U. K.

Saager, P. M., H. J. W. Debaar, and R. J. Howland (1992), Cd, Zn, Ni and Cu in the Indian Ocean, *Deep Sea Res., Part A*, 39(1), 9–35.

Scheffel, A., N. Poulsen, S. Shian, and N. Kröger (2011), Nanopatterned protein microrings from a diatom that direct silica morphogenesis, *Proc. Natl. Acad. Sci. U. S. A.*, 108(8), 3175–3180, doi:10.1073/pnas.1012842108.

Schmidt, A., M. Gube, and E. Kothe (2009), In silico analysis of nickel containing superoxide dismutase evolution and regulation, *J. Basic Microbiol.*, 49(1), 109–118, doi:10.1002/jobm.200800293.

Sclater, F. R., E. Boyle, and J. M. Edmond (1976), On the marine geochemistry of nickel, *Earth Planet. Sci. Lett.*, 31(1), 119–128, doi:10.1016/0012-821X(76)90103-5.

Selph, K. E., M. R. Landry, A. G. Taylor, E. J. Yang, C. I. Measures, J. J. Yang, M. R. Stukel, S. Christensen, and R. R. Bidigare (2011), Spatially resolved taxon-specific phytoplankton production and grazing dynamics in relation to iron distributions in the equatorial Pacific between 110 and 140°W, *Deep Sea Res., Part II*, 58(3–4), 358–377, doi:10.1016/j.dsr2.2010.08.014.

Sheng, G., S. Yang, J. Sheng, J. Hu, X. Tan, and X. Wang (2011), Macroscopic and microscopic investigations of Ni(II) sequestration on diatomite by batch, XPS, and EXAFS techniques, *Environ. Sci. Technol.*, *45*, 7718–7726, doi:10.1021/es202108q.

Sumper, M., and N. Kröger (2004), Silica formation in diatoms: The function of long-chain polyamines and silaffins, *J. Mater. Chem.*, *14*(14), 2059–2065, doi:10.1039/b401028k.

Sunda, W., D. J. Kieber, R. P. Kiene, and S. Huntsman (2002), An antioxidant function for DMSP and DMS in marine algae, *Nature*, *418*(6895), 317–320, doi:10.1038/nature00851.

Twining, B. S., S. B. Baines, N. S. Fisher, J. Maser, S. Vogt, C. Jacobsen, A. Tovar-Sanchez, and S. A. Sanudo-Wilhelmy (2003), Quantifying trace elements in individual aquatic protist cells with a synchrotron x-ray fluorescence microprobe, *Anal. Chem.*, *75*(15), 3806–3816, doi:10.1021/ac034227z.

Twining, B. S., S. B. Baines, and N. S. Fisher (2004), Element stoichiometries of individual plankton cells collected during the Southern Ocean Iron Experiment (SOFeX), *Limnol. Oceanogr.*, *49*(6), 2115–2128, doi:10.4319/lo.2004.49.6.2115.

Twining, B. S., D. Nunez-Milland, S. Vogt, R. S. Johnson, and P. N. Sedwick (2010), Variations in *Synechococcus* cell quotas of phosphorus, sulfur, manganese, iron, nickel, and zinc within mesoscale eddies in the Sargasso Sea, *Limnol. Oceanogr.*, *55*(2), 492–506, doi:10.4319/lo.2009.55.2.0492.

Twining, B. S., S. B. Baines, J. B. Bozard, S. Vogt, E. A. Walker, and D. M. Nelson (2011), Metal quotas of plankton in the equatorial Pacific Ocean, *Deep Sea Res., Part II*, *58*, 325–341, doi:10.1016/j.dsr2.2010.08.018.

Vrieling, E. G., W. W. C. Gieskes, and T. P. M. Beelen (1999), Silicon deposition in diatoms: Control by the pH inside the silicon deposition vesicle, *J. Phycol.*, *35*(3), 548–559, doi:10.1046/j.1529-8817.1999.3530548.x.

Wolfe-Simon, F., D. Grzebyk, O. Schofield, and P. G. Falkowski (2005), The role and evolution of superoxide dismutases in algae, *J. Phycol.*, *41*(3), 453–465, doi:10.1111/j.1529-8817.2005.00086.x.